JOURNAL OF SOLID STATE CHEMISTRY 116, 224–231 (1995)

$LaCoO_3$ Revisited

M. A. Señarís-Rodríguez and J. B. Goodenough[1]

Center for Materials Science and Engineering, ETC 9.102., University of Texas at Austin, Austin, Texas 78712-1063

Received June 30, 1994; accepted August 12, 1994

Homogeneous samples of $LaCoO_3$ were prepared from coprecipitated precursors; they reveal that single-phase samples are restricted to a narrow range of the [La]/[Co] ratio of about 1.0. A first-order phase change near 1200 K only appears where Co_3O_4 is present as an impurity phase. Evolution with temperature from all low-spin Co(III) at $T = 0$ K to 50% high-spin Co^{3+} and 50% intermediate-spin Co(III) above 650 K is monitored with magnetic susceptibility, resistance, and thermopower measurements. Evidence is found for a dynamic ordering of high-spin Co^{3+} and low-spin Co(III) in the intermediate-temperature interval 110 K $< T <$ 350 K. The lifetime of a Co^{3+} ion decreases with increasing temperature to a $\tau < 10^{-8}$ sec for $T > 200$ K. The intermediate-temperature phase is semiconductive with an $E_g \approx 0.14$ eV for excitations of hole-electron pairs. The holes are mobile; the electrons are trapped as Co^{2+} on high-spin sites until they recombine with a mobile hole. The metallic high-temperature phase for $T >$ 650 K is nucleated and grows with increasing temperature in the interval 350 K $< T <$ 650 K.

INTRODUCTION

Early work on $LaCoO_3$ established the existence of a transition from low-spin Co(III) to mostly high-spin Co^{3+} with increasing temperature over the interval 0 K $< T <$ 650 K (1–7). However, at that time samples were prepared by high-temperature ceramic techniques, which made it difficult to control sample homogeneity and oxygen stoichiometry. Consequently a subtle interpretation of the evolution with temperature of the magnetic, structural, and transport properties that was proposed (6) has since been debated by several groups (8–20) on the basis of data that have varied somewhat from laboratory to laboratory.

Four principal issues have been in contention:

(i) Are the localized spins evident at temperatures $T <$ 35 K intrinsic to $LaCoO_3$ or are they due to impurities and/or bulk defects? If they are intrinsic, are they confined to the surface of the $LaCoO_3$ particles?

(ii) Is there a temperature domain within which the high-spin Co^{3+} and low-sin Co(III) configurations become ordered, short-range, or long-range, on alternate Co ions of the structure; and if so, what is this temperature interval?

(iii) Does disproportionation of trivalent cobalt into divalent and tetravalent cobalt occur, and if so, to what extent and in what temperature interval?

(iv) Is the observation of a first-order phase transition near 1200 K, first reported for an apparently single-phase sample of $LaCoO_3$, due to a Co_3O_4 impurity phase?

We report in this paper the magnetic and transport properties of single-phase $LaCoO_3$ prepared from a coprecipitated precursor to ensure homogeneity; the samples were analyzed thermogravimetrically and chemically to ensure a stoichiometric oxygen content over the entire temperature range 0 K $< T <$ 1173 K.

Our data distinguish the following temperature domains:

(i) 0 K $< T <$ 35 K: The bulk cobalt are essentially all low-spin Co(III), but localized spins associated with surface cobalt order so as to give a weak ferromagnetism at 5 K.

(ii) 35 K $< T <$ 110 K: The concentration of thermally excited high-spin Co^{3+} configurations increases smoothly with temperature, but the coordination of each high-spin Co^{3+} ion by low-spin Co(III) near neighbors resticts the ratio of high-spin to total bulk cobalt to $[Co^{3+}]/[Co] < 0.5$.

(iii) 110 K $< T <$ 350 K: A mixture of approximately 50% high-spin and 50% low-spin cobalt forms an ordered semiconductive phase that inhibits the further creation of high-spin Co^{3+} ions in this temperature interval; supplementary data from the literature are interpreted to indicate that the ordering is short range with configuration fluctuations at a high-spin Co^{3+} ion having a lifetime that decreases with increasing temperature from $\tau > 10^{-8}$ sec at $T <$ 200 K to $\tau < 10^{-8}$ sec at $T >$ 200 K.

(iv) 350 K $< T <$ 650 K: A metallic phase coexists with the dynamically ordered semiconductive phase, and a smooth change in physical properties occurs on crossing the percolation threshold for the metallic phase near 450 K.

(v) $T \geq 650$ K: A homogeneous metallic phase contains, at 650 K, high-spin cobalt alternating with intermediate-

[1] To whom correspondence should be addressed.

0022-4596/95 $6.00

spin cobalt ions in an ordered array; the metallic conduction is attributed to a transition from fluctuating, localized Co-3*d* configurations in the semiconductive phase to itinerant σ^* states in the metallic phase.

In addition, supplementary data from the literature indicate that the two distinguishable cobalt arrays persist to at least 800 K. Finally, the first-order phase change reported to occur near 1200 K is due to a Co_3O_4 impurity phase that segregates where a ratio [La]/[Co] < 1 exists, which implies that segregation can occur in cobalt-rich regions in inhomogeneous samples having an overall stoichiometric ratio [La]/[Co] = 1.

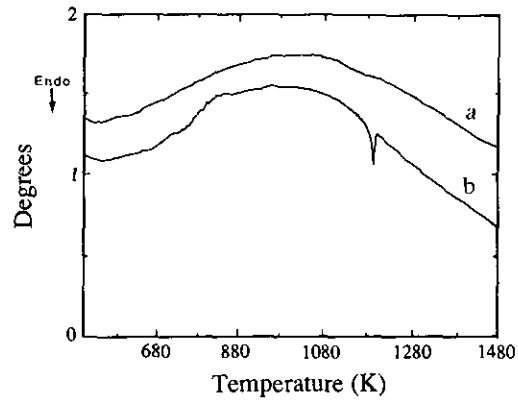

FIG. 1. DTA results of (a) single-phase $LaCoO_3$ and (b) a cobalt-rich sample containing Co_3O_4 as a second phase.

EXPERIMENTAL

La and Co species were coprecipitated with a carefully controlled [La]/[Co] ratio that was varied from 0.9 to 1.1. The starting materials were La_2O_3 and $Co(NO_3)_2 \cdot 6H_2O$.

The cobalt nitrate was first dissolved in water, and the cobalt content in the solution was determined gravimetrically with anthranilic acid as the precipitating agent. Known volumes of this cobalt solution were then mixed with the appropriate volumes of a lanthanum nitrate solution obtained by dissolving weighed amounts of dry La_2O_3 in nitric acid. Coprecipitation at pH 11 was achieved by adding aqueous solutions of KOH and K_2CO_3 as precipitating agents. The precipitate was carefully washed, dried, and then decomposed at 750°C. The decomposition precursor powder was pressed into pellets that were heated at 1000°C for 72 hr to obtain stoichiometric $LaCoO_3$ as well as both La-rich and Co-rich products.

The product materials were examined by X-ray powder diffraction and electron diffraction. Iodometric titrations were carried out to determine the oxygen content in the sample with [La]/[Co] = 1. The thermal stability of all the materials was checked by differential thermal analysis (DTA) and thermogravimetric analysis (TGA), with a Perkin–Elmer thermal analysis system.

Magnetic susceptibilities of sintered pellets were obtained in a field H = 10 kOe from 4.2 to 380 K and H = 5 kOe from 380 to 750 K with a Quantum Design MPMS SQUID magnetometer.

Four-probe electrical resistance of pressed pellets was measured in the range 4.2 K $\leq T \leq$ 823 K in a homemade device equipped with a Lakeshore temperature controller.

Seebeck coefficients of pressed pellets were measured in the temperature interval 4.2 K $\leq T \leq$ 823 K in a homemade device described elsewhere (21).

RESULTS

Variation of the [La]/[Co] ratio from 0.9 to 1.1 was monitored by room temperature X-ray powder diffraction and thermal analysis. X-ray diffraction revealed second phases with only a small deviation from 1.0 of the [La]/[Co] ratio. The cobalt-rich products contained cobalt oxides, which were mainly Co_3O_4; the lanthanum-rich products contained lanthanum hydroxycarbonate.

The DTA data, see Fig. 1, showed an endothermic peak at 1190 K only in those samples containing Co_3O_4 as a second phase, which confirms the conclusion of Thornton *et al.* (9) that the first-order transition originally reported (6) for nominal $LaCoO_3$ was due to the presence of a Co_3O_4 impurity and is not an intrinsic property of $LaCoO_3$.

The TGA data showed a small weight loss in the temperature interval 493 K < T < 573 K. The subtle exothermic features appearing in the DTA curves of Fig. 1 in the same temperature range were present in all samples studied; these features and the weight loss are assumed to signal loss of bound water and/or CO_2 from the surface. A reconstruction of the surface above 573 K would stabilize tetrahedral-site, or fivefold coordinated high-spin cobalt; Richter *et al.* (14) have presented direct evidence for high-spin cobalt in the surface layer of $LaCoO_3$. A surface Co^{2+} ion in a tetrahedral or fivefold coordination would be susceptible to attack by O_2 molecules, and the resulting active surface oxygen would give a high activity for CO oxidation on $LaCoO_3$ as reported by Voorhoeve *et al.* (22).

Iodometric titrations carried out in the single-phase $LaCoO_3$ material confirmed that the sample has the right oxygen stoichiometry.

Electron diffraction micrographs obtained along different zone axes of this single-phase sample showed only the reflections expected for a rhombohedral ($R\bar{3}c$) perovskite with a = 5.378 Å and α = 60.8° in agreement with a neutron-diffraction refinement (10).

Figure 2 shows the temperature dependence of the molar magnetic susceptibility χ_m below 400 K for stoichiometric, cobalt-rich, and lanthanum-rich $LaCoO_3$; the influence of quenching from 1000°C and of repeated

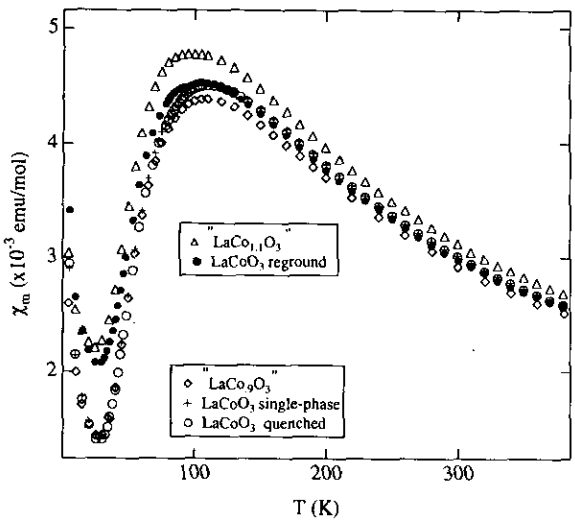

FIG. 2. Temperature dependence of the molar magnetic susceptibility of samples with "nominal" composition $LaCo_{1-x}O_3$ ($-0.1 \leq x \leq 0.1$) measured at $H = 10$ kOe in the temperature interval 4.2 K $< T <$ 380 K.

regrinding and refiring of stoichiometric $LaCoO_3$ is also shown. There is no bulk long-range magnetic order (1, 10). The maximum in χ_m versus temperature near 110 K reflects a conversion of the remaining high-spin Co^{3+} ions in bulk $LaCoO_3$ to diamagnetic low-spin Co(III) ions on cooling below 110 K. The sharp minimum in χ_m versus temperature at $T \approx 35$ K reflects the retention of some high-spin cobalt ions to lowest temperatures; these give a weak ferromagnetic signal at 5 K that appears to be associated with the surface layer. The deepest minimum in χ_m at $T \approx 35$ K is found in as-prepared samples with and without the presence of lanthanum hydroxycarbonate as a second phase. The introduction of the spinel phase Co_3O_4, which contains high-spin Co^{2+} in tetrahedral sites, adds to the magnetic susceptibility at all temperatures measured (up to 750 K) and raises the minimum value of χ_m at $T \approx 35$ K. The lowest susceptibility at all temperatures is found for the sample having a little lanthanum hydroxycarbonate present as a detectable second phase, which indicates that the concentration of localized spins that are intrinsic to single-phase $LaCoO_3$ is a minimum at the La-rich boundary of the phase field. This deduction is consistent with the hypothesis that the localized magnetic moments are associated with surface cobalt, perhaps present as Co^{2+} ions in a reconstructed cobalt-rich surface region. If this hypothesis is correct, then we might expect to see the volume of this surface region increased upon regrinding the as-prepared sample. Indeed, Fig. 2 shows that regrinding a single-phase $LaCoO_3$ sample increases χ_m below 100 K; below 35 K the increase is even greater than in the cobalt-rich sample with Co_3O_4 as a detected second phase. We conclude that localized cobalt magnetic moments in single-phase $LaCoO_3$ are intrinsic to a reconstructed surface of the $LaCoO_3$ particles. In further support of this conclusion, we note that measurement of the susceptibility on heating to 750 K is not completely reversible on cooling; a reconstruction of the surface above 400 K on loss of bound surface water and/or CO_2 results in a change in the χ_m versus T curve that is consistent with creation of surface Co^{2+} ions.

The plot of inverse susceptibility (χ_m^{-1}) versus temperature shown in Fig. 3 is similar to that already reported in the literature. In this plot the minimum in χ_m at $T \approx 35$ K appears as a sharp maximum, and the maximum in χ_m at $T \approx 110$ K appears as a minimum. What is of particular interest in this plot is the existence of two temperature domains in which χ_m^{-1} increases nearly linearly with temperature in a typical Curie–Weiss behavior; these two temperature regions are separated by a domain in which χ_m^{-1} versus T exhibits a plateau. The plateau indicates a temperature interval where there is a conversion from one "stable" spin configuration at the cobalt ions to another, but there appears to be nothing significant about the plateau character in the interval 450 K $< T <$ 650 K; in fact, the shape of the curve in the transition region depends only on how abruptly the Curie and Weiss constants are changing through the transitional interval. $YCoO_3$, for example, exhibits a transition between two Curie–Weiss temperature domains where the χ_m^{-1} versus T curve exhibits a negative slope (23).

We may deduce something about the character of the two relatively stable spin-state configurations on either side of the plateau from the apparent Curie constant C and Weiss constant θ obtained from the two Curie–Weiss temperature domains. By fitting the straight-line segments

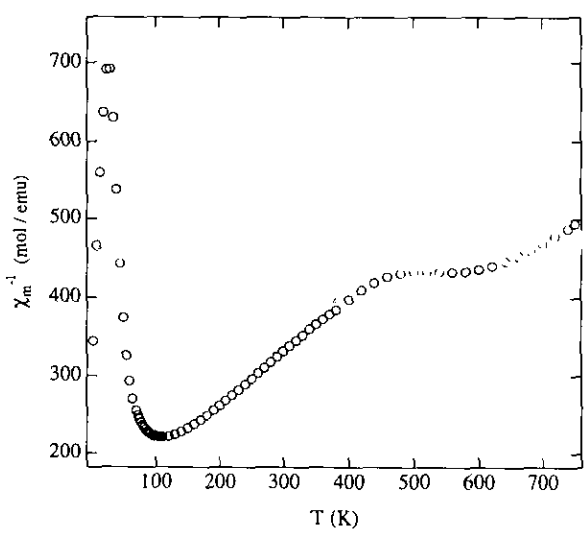

FIG. 3. Inverse molar magnetic susceptibility versus T plot of single-phase $LaCoO_3$ in the temperature range 4.2 $< T <$ 750 K ($H = 10$ kOe).

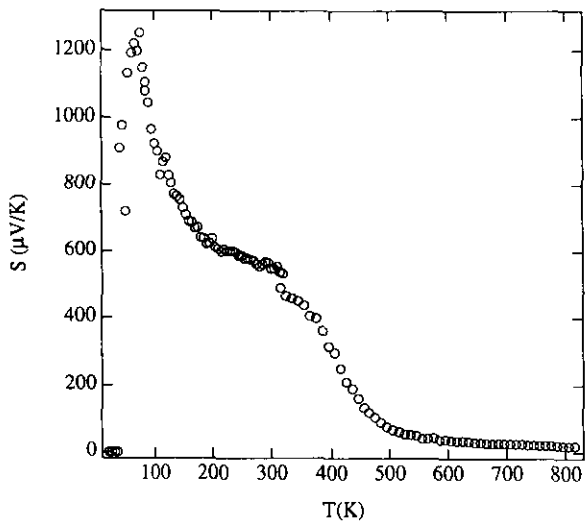

FIG. 4. Temperature dependence of the Seebeck coefficient of single-phase $LaCoO_3$ (4.2 K $< T <$ 823 K). The step at room temperature is due to a change in measurement apparatus.

in those two temperature domains, we obtain for pure $LaCoO_3$ a $\mu_{eff} = \sqrt{8C}\ \mu_B = 3.4\ \mu_B$ and a $\theta = -185$ K for 150 K $< T <$ 350 K and a $\mu_{eff} = 4.1\ \mu_B$ with $\theta = -504$ K for $T > 650$ K. A $\mu_{eff} = 4.9\ \mu_B$ is predicted for an all-high-spin phase if the orbital contribution to the moment is neglected; a $\mu_{eff} = 4.0\ \mu_B$ for 50:50% high-spin and intermediate-spin (t^5e^1) states, and a $\mu_{eff} = 3.5\ \mu_B$ for 50% high-spin and 50% low-spin states. The slope of χ_m^{-1} versus T curve in the interval 150 K $< T <$ 350 K is clearly consistent with a 50% Co^{3+} and 50% Co(III) configuration while that for $T > 650$ K is consistent with a 50% high-spin and 50% intermediate-spin configuration on trivalent cobalt ions. A 50% high-spin and 50% lower-spin configurations on alternate cobalt ions of the simple-cubic cobalt-ion array would be stabilized by a cooperative displacement of the oxide ions away from the high-spin cobalt and toward the lower-spin cobalt (2). Moreover coupling between Co^{3+} ions across diamagnetic Co(III) would give a smaller Weiss constant $\theta = CW$, where W is the Weiss molecular-field coefficient, than the stronger coupling with intermediate-spin near neighbors.

The Seebeck coefficient, Fig. 4, increases from $\alpha = 0$ at $T = 4.2$ K to a very large positive value at $T = 75$ K; it has a $1/T$ dependence in the range 75 K $< T <$ 310 K, but it remains high ($\alpha > 550\ \mu$V/K) throughout this interval. This observation indicates that only holes are mobile in the intermediate, semiconductive phase. In the interval 350 K $< T <$ 600 K α decreases more strongly with increasing temperature through the transition to the high-temperature, metallic phase at $T > 650$ K where α is small and still positive up to the highest temperature measured (823 K).

For the intermediate-temperature phase, we assume that the $\alpha \sim 1/T$ dependence represents a phase having a fixed activation energy $E_g \gg kT$ for the creation of mobile holes and trapped electrons. If the mobile holes are small polarons, an

$$\alpha - \alpha_0 \approx -\frac{k}{e}\ln\left(\frac{1-p}{p}\right) \approx \frac{E_g}{2eT} \qquad [1]$$

allows calculation of the energy gap E_g. This energy gap is to be distinguished from the energy Δ required to transform a low-spin Co(III) into the high-spin state. To obtain the motional enthalpy of the small-polaron holes with mobility

$$\mu_p = \frac{eD_0}{kT}\exp\left(-\Delta G_m/kT\right), \qquad [2]$$

we use the conductivity expression

$$\sigma = pe\mu_p \sim T^{-1}\exp\left(-E_a/kT\right), \qquad [3]$$

with $E_a = \Delta H_m + (E_g/2)$ and $\Delta G_m = \Delta H_m - T\Delta S_m$. For small polarons, the mobile hole density is $p = p_0 \exp(-E_g/2kT)$ with p_0 independent of temperature, and

$$\ln\left(T/R\right) = \text{const} - \left(E_a/kT\right), \qquad [4]$$

where R is the measured resistance. From Eqs. [1] and [4] and Fig. 5a, we obtain $E_g = 0.14$ and 0.10 eV and $\Delta H_m = 0.08$ and 0.05 eV for the intermediate-temperature ranges 110 K $< T <$ 240 K and 260 K $< T <$ 310 K, respectively. Between 400 and 650 K, the resistance R decreases in a smooth transition toward a metallic temperature dependence, see Fig. 5(b).

DISCUSSION

Goodenough (2) pointed out in an early paper that the cubic perovskite structure can support the stabilization of a phase in which alternate trivalent cobalt ions have high-spin and low-spin configurations; it would be stabilized by a cooperative displacement of the oxygen ions toward the low-spin Co(III) and away from the high spin Co^{3+} ions. This ordering could be either long-range and static or short-range and dynamic. Raccah and Goodenough (6) interpreted the data above room temperature in terms of an intermediate-temperature stabilization of such an ordered state. Bhide *et al.* (8) subsequently found direct evidence from Mössbauer data for the two states of cobalt, but with a ratio $[Co^{+3}]/[Co]$ versus temperature exhibiting a sharp maximum at 200 K. Although the actual concentrations of Co^{3+} versus Co(III) obtained from this analysis do not appear to be quantitative, a maximum in the Co^{3+} concentration at 200 K is clearly

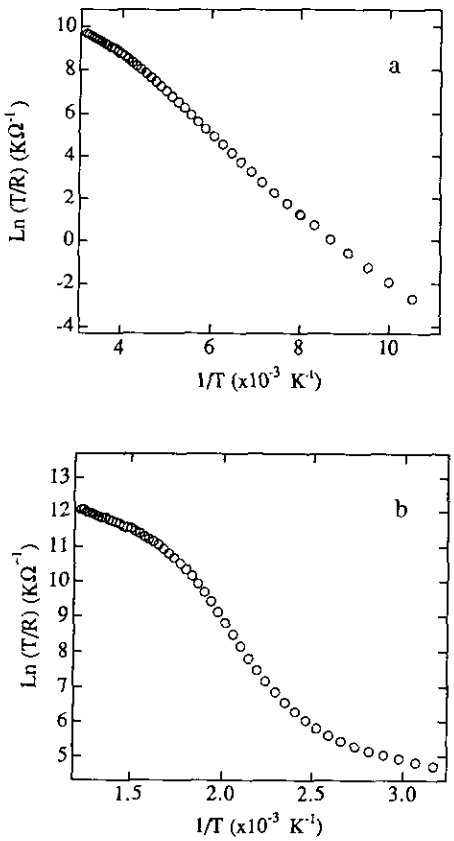

FIG. 5. Plots of $\ln (T/R)$ versus T^{-1} corresponding to the single-phase $LaCoO_3$ material: (a) Low temperature interval: 80 K $\leq T \leq$ 300 K. (b) High temperature interval: 300 K $\leq T \leq$ 823 K.

at variance with the susceptibility data. The apparent decrease in $[Co^{3+}]$ with $T > 200$ K was attributed to the transfer of an e_g electron from the Co^{3+} to a neighboring Co(III); but the subsequent creation of low-spin Co(II) and intermediate-spin Co(iv) in the concentration required by the Mössbauer data is not compatible with the transport data of Figs. 4 and 5. An alternative explanation for the apparent decrease in $[Co^{3+}]$ with increasing $T > 200$ K observed by Mössbauer spectroscopy is an increase with temperature in the fluctuation rate of a *dynamic ordering* between Co^{3+} and Co(III), the lifetimes of the Co^{3+} ions decreasing from $\tau > 10^{-8}$ sec below 200 K to $\tau < 10^{-8}$ sec above 200 K.

Independent evidence for a stable $[Co^{3+}]/[Co]$ ratio persisting over the range 110 K $< T <$ 350 K comes from the neutron-scattering data of Asai *et al.* (12), which clearly established the presence of a temperature-induced magnetic moment on the cobalt that increases smoothly, but sharply with temperature between 35 and 100 K before saturating from 110 K to room temperature. Since a stabilization of 50% high-spin and 50% low-spin cobalt is physically understandable and since the susceptibility data are compatible with a 50% Co^{3+}: 50% Co(III) configuration, we conclude that this ratio of spin states is stabilized by a dynamic ordering of the high-spin and low-spin states. Moreover, the transport data show that $LaCoO_3$ is a semiconductor with a large, positive Seebeck coefficient in this temperature interval. An ordering, dynamic or static, of 50% Co^{3+} and 50% Co(III) spin states allows interpretation of the transport data as is illustrated by the energy diagrams of Fig. 6.

Figure 6a represents the low-spin phase at $T = 0$ K. In this phase, the covalent component of the Co–O bonding is strong enough to transform the σ-bonding orbitals of e parentage into an empty, antibonding σ^* band; strong hybridization of the cobalt orbitals of t_2 parentage with the O-2p orbitals also creates antibonding π^* band states at the top of the valence band. This phase is a diamagnetic insulator.

Figure 6b illustrates the intermediate-temperature phase where the ordering of Co(III) and Co^{3+} spin states is postulated to occur. The $Co^{3+}: 3d^6$ configurations are assumed to be localized whereas the Co(III) ions are described by coupled $(CoO_6)^{9-}$ molecular-cluster orbitals in which the highest occupied orbitals are the π^* molecular-cluster states. Intraatomic exchange lifts the spin degeneracy of the Co^{3+} ion configuration, stabilizing majority-spin (α-spin) states relative to the minority-spin (β-spin) states. Removal of the spin degeneracy by the intraatomic-exchange stabilization makes the sum of the one-electron energies for the high-spin state nearly the same as that for the low-spin state, which is why crossover from the low-spin to the high-spin state occurs at modest temperatures. In the high-spin $Co^{3+}: t_\alpha^3 t_\beta^1 e_\alpha^2$ localized configuration, the occupied t_β^1 state is separated from the empty t_β^2 state by an on-site electron–electron coulomb energy U_t. Excitation of an electron across the energy gap E_g from the π^* molecular-cluster states to an acceptor t_β^2 state at a Co^{3+} ion creates a trapped electron at a localized $Co^{2+}: 3d^7$ configuration and a mobile hole in the covalent π^* bands of the Co(III)–O array. Since only the holes are mobile, the Seebeck coefficient α is positive; the excited electrons remain trapped until they recombine with a mobile hole. Since the π^* bands are narrow, the holes form small polarons, so α has a large magnitude as described by Eq. [1].

Extended X-ray absorption fine structure (EXAFS) measurements (18) detected only a single Co–O distance of 1.92 Å at room temperature and at 400 K, but in the interval 523 K $\leq T \leq$ 800 K two distances were resolved, 1.66 and 2.20Å. Failure to detect two distinguishable Co–O distances in the range 295 K $\leq T \leq$ 400 K is consistent with our interpretation of the Mössbauer data; the dynamic fluctuations of the ordered state are too rapid for EXAFS to resolve the two Co–O distances associated, respectively, with Co^{3+} and Co(III) ions. Since the two

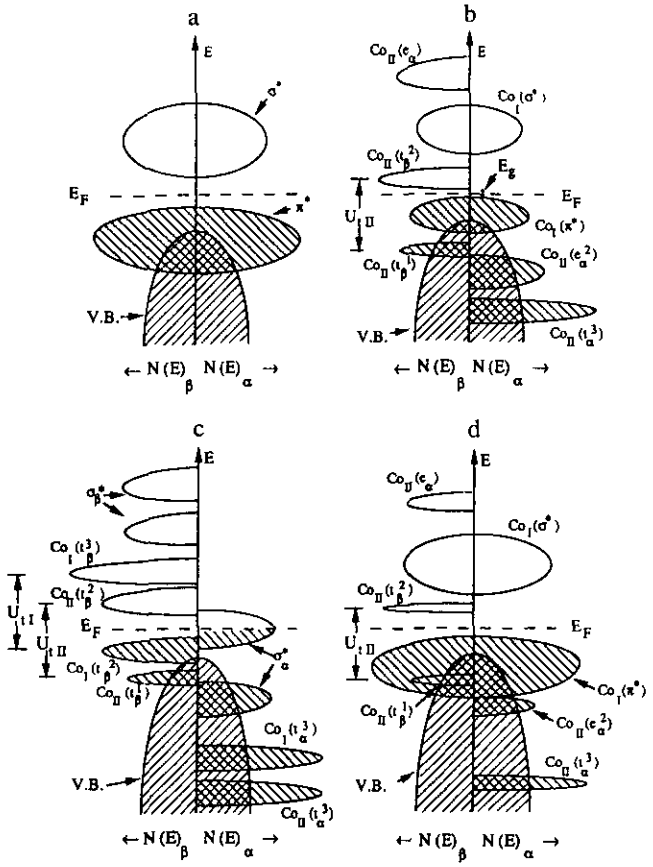

FIG. 6. Schematic representation of the evolution of the electronic structure of $LaCoO_3$ with temperature. (a) Low-spin phase at $T = 0$ K. (b) Intermediate-temperature ordered phase present in the interval 110 K $< T <$ 350 K consisting of 50% Co(III) : 50% Co^{3+} (frozen picture). Co_I: low-spin Co(III) ions, Co_{II}: high-spin Co^{3+} ions. (c) Metallic phase present at $T >$ 650 K consisting of 50% Co(iii) : 50% Co^{3+}. Co_I: intermediate-spin Co(iii) ions, Co_{II}: high-spin Co^{3+} ions. (d) Transition from the low-spin to the 50% Co(III) : 50% Co^{3+} phase ocurring in the temperature interval 0 K $< T <$ 110 K.

spin states would be differentiated by a cooperative breathing-mode displacement of the oxygen ions, fluctuations between the two spin states at optical-mode vibrational frequencies can be anticipated. In fact, a vibronic resonance between the two equilibrium Co–O distances associated with the two spin states might be responsible for stabilizing the intermediate-temperature phase above 200 K. On the other hand, the observation (18) of two distinguishable Co–O distances above 523 K with a 50% occupation at $T \approx 650$ K signals that two distinguishable cobalt-ion arrays are present in the metallic phase at least to 800 K. This observation signals an ordering of 50% high-spin Co^{3+} and a 50% lower-spin state; the magnetic-susceptibility data indicate that the lower-spin state is an intermediate-spin Co(iii) ion. As is illustrated in Fig. 6c, it is the conversion of low-spin Co(III) to intermediate-spin Co(iii) that makes possible a transition from the semiconductive phase to a metallic phase. The metallic phase is not stabilized by a vibronic coupling between the two equilibrium Co–O distances, one longer and the other shorter, so the cooperative oxide-ion displacements become quasistatic and just observable at 650 K by a diffraction experiment (10) as a lowering of the symmetry from $R\bar{3}c$ to $R\bar{3}$ (6).

In Fig. 6c, the two distinguishable cobalt ions correspond to the intermediate-spin Co_I(iii) and the high-spin Co_{II}^{3+} ions. The Fermi energy E_F lies between the localized-electron filled $Co_I : t_\beta^2$ and empty $Co_{II} : t_\beta^2$ manifolds; these manifolds are split by an on-site coulomb energy U_t from, respectively, an empty $Co_I : t_\beta^3$ and a filled $Co_{II} : t_\beta^1$ energy level. The itinerant-electron σ_α^* and σ_β^* bands are split in two by the translational symmetry, and E_F lies in the middle of the upper σ_α^* band. The density of σ_α^* holes would be associated with the more covalently bonded Co_I ions. The partially filled σ_α^* band is responsible for the p-type conductivity above 650 K.

The transition from the low-spin phase of Fig. 6a to the intermediate-temperature phase of Figure 6b would progress via an increase in the density of high-spin states at the expense of the density of low-spin states as indicated in Fig. 6d. The only constraint on the transformation is that every high-spin Co^{3+} be coordinated by low-spin Co(III) as a result of a cooperative displacement of oxide ions away from the Co^{3+} ions toward the neighboring Co(III) ions. It is this constraint that ultimately stabilizes the 50% ordered phase over a finite temperature range. Excitation of electrons from the π^* band to the localized t_β^2 state becomes more probable as the density of empty t_β^2 states at high-spin Co^{3+} increases, but the activation energy $E_g/2$ can be expected to remain essentially constant over the interval 110 K $< T <$ 350 K. The change in E_g observed near 250 K coincides with the rapid decrease in Co^{3+} Mössbauer signal; it suggests an important change in the electron-lattice interaction.

The transition from the semiconductive to the metallic phase would occur via a two-phase mixture in which domains of the metallic phase are nucleated and grow with increasing temperature at the expense of the semiconductive phase. Such an evolution can account for the smooth transition from semiconductive to metallic properties that is observed.

Finally, we comment on the evidence for a spin-state transition from electron spectroscopy. The first point to note is the lack of any evidence for valence states other than trivalent cobalt. This finding is in agreement with the present discussion; in the semiconductor phase, the thermal excitation of electron-hole pairs gives only small concentrations of divalent and tetravalent cobalt. Earlier speculations about electron-transfer reactions creating substantial concentrations of polar states on the cobalt-ion array appear to be ruled out. Veal and Lam (13) found

evidence in the X-ray photoelectron spectra for high-spin Co^{3+} at room temperature with an apparent increase in population at 573 K. The presence of multiplets corresponding to the high-spin state was observed (15) in the He II spectra of $LaCoO_3$ already at 77 K. Masuda *et al.* (17) found evidence in their electron-emission spectrum, obtained from thermal collisions of He* ions with $LaCoO_3$, for the presence of both high-spin and low-spin cobalt at room temperature. In contrast to those reports, Abbate *et al.* (19) found no evidence for high-spin cobalt below 420 K in their X-ray absorption data; however, their analysis has been criticized for being based on a purely ionic model (20). Instead, Barman and Sarma (20) have used a configuration–interaction model to interpret the valence-band and Co-2*p* photoemission spectra of $LaCoO_3$ obtained at 150, 300, and 573 K; these authors obtained a 30% Co^{3+} : 70% Co(III) population at 100 K that changed little to 420 K; it appeared to increase to 50% high-spin: 50% lower-spin state at 573 K. In view of the apparent uncertainties in the development of a quantitative interpretation of the electron-spectroscopy data, we conclude that these data are consistent with the model we have proposed here.

CONCLUSIONS

A model is proposed that appears to resolve the outstanding questions concerning the character of the transition with increasing temperature from low-spin Co(III) to high-spin Co^{3+} in $LaCoO_3$. The following issues are addressed:

(i) Sample preparations from coprecipitated precursors have permitted the synthesis of homogeneous products. In air, oxygen stoichiometry is retained up to 1173 K. These preparations reveal that single-phase $LaCoO_3$ is restricted to a narrow range of [La]/[Co] about 1.0. Excess La results in the appearance of diamagnetic lanthanum hydroxycarbonate as a second phase; excess cobalt results is the appearance of magnetic cobalt oxides. In agreement with Thornton *et al.* (9), the first-order phase change near 1210 K reported for $LaCoO_3$ samples prepared by conventional ceramic techniques is due to a Co_3O_4 impurity phase resulting from chemical inhomogeneity.

(ii) The bulk Co(III) are all low-spin at lowest temperatures. However, retention of some localized spins at surface cobalt ions, probably tetrahedral-site Co^{2+} ions, is responsible for a deep minimum in χ_m versus temperature at $T \approx 35$ K in single-phase $LaCoO_3$; this minimum becomes more shallow with the introduction of magnetic impurities and/or defects.

(iii) In the temperature interval $0 \text{ K} < T < 100$ K, more and more high-spin Co^{3+} ions are created; each of these Co^{3+} is coordinated by six low-spin Co(III) near neighbors. The larger volume of Co^{3+} ions is accommodated by a cooperative motion of the coordinating oxygen ions away from the high-spin cations toward the near-neighbor low-spin Co(III). The limiting number of Co^{3+} ions that can be accommodated with this constraint is an ordered 50% high-spin and 50% low-spin phase.

(iv) In the range $110 \text{ K} < T < 350$ K, the ordered phase is stabilized as a distinguishable intermediate-temperature phase. However, the order between Co(III) and Co^{3+} ions is not static but dynamic, and it may couple strongly with the lattice vibration modes at $T \geq 250$ K.

(v) Throughout the interval $110 \text{ K} < T < 350$ K, excitation of electrons from a narrow valence band to localized t_β^2 states at high-spin sites introduces mobile small-polaron holes and trapped electrons at stationary Co^{2+} ions; this semiconductive temperature interval is characterized by a large, positive Seebeck coefficient that decreases as $1/T$.

(vi) There is no evidence of larger concentrations of Co(iv) and Co(II) ions at higher temperatures created by charge transfer of an e_g electron from a Co^{3+} ion to a Co(III) ion; rather a metallic phase containing 50% high-spin Co^{3+} and 50% intermediate-spin Co(iii) ions is stabilized at higher temperatures.

(vii) In the range $350 \text{ K} < T < 650$ K, a smooth semiconductor to metal transition occurs as the metallic phase is nucleated within the dynamically ordered phase and grows with increasing temperature; the percolation limit for the metallic phase is reached near 450 K.

(viii) The metallic phase stable above 650 K is characterized by two Co–O separations to at least 800 K; nearly equal population of the two bond lengths at 650 K signals a quasistatic ordering of high-spin Co^{3+} and intermediate-spin Co(iii) on the two cobalt subarrays of the metallic phase.

ACKNOWLEDGMENTS

The authors thank the Ministerio de Educación y Ciencia of Spain and the Fulbright Commission for the grant of MASR and the Robert A. Welch Foundation of Houston, TX (Grant F-1066) and the National Science Foundation (Grant DMR-9223552) for the remaining support.

REFERENCES

1. W. C. Koehler and E. O. Wollan, *J. Phys. Chem. Solids* **2,** 100 (1957).
2. J. B. Goodenough, *J. Phys. Chem. Solids* **6,** 287 (1958).
3. R. R. Heikes, R. C. Miller, and R. Mazelsky, *Physica* **30,** 1600 (1964).
4. C. S. Naiman, R. Gilmore, B. Di Bartolo, A. Linz, and R. Santoro, *J. Appl. Phys.* **36,** 1044 (1965).
5. G. H. Jonker, *J. Appl. Phys.* **37,** 1424 (1966).
6. P. M. Raccah and J. B. Goodenough, *Phys. Rev.* **155,** 932 (1967).
7. N. Menyuk, K. Dwight, and P. M. Raccah, *J. Phys. Chem. Solids* **28,** 549 (1967).

8. V. G. Bhide, D. S. Rajoria, G. R. Rao, and C. N. R. Rao, *Phys. Rev. B* **6** 1021 (1972).
9. G. Thornton, B. C. Tofield, and D. E. Williams, *Solid State Commun.* **44,** 1213 (1982).
10. G. Thornton, B. C. Tofield, and A. W. Hewat, *J. Solid State Chem.* **61,** 301 (1986).
11. G. Thornton, F. C. Morrison, S. Partington, B. C. Tofield, and D. E. Williams, *J. Phys. C: Solid State Phys.* **21,** 2871 (1988).
12. K. Asai, P. Gehring, H. Chou, and G. Shirane, *Phys. Rev. B* **40**(16) 10982 (1989).
13. V. W. Veal and D. J. Lam, *J. Appl. Phys.* **49,** 1461 (1978).
14. L. Richter, S. D. Bader, and M. B. Brodsky, *Phys. Rev. B* **22,** 3059 (1980).
15. A. F. Orchard and G. Thornton, *J. Electron Spectrosc. Relat. Phenom.* **22,** 271 (1981).
16. G. Thornton, I. W. Owen, and G. P. Diakun, *J. Phys. Condens. Matter* **3,** 417 (1991).
17. S. Masuda, M. Aoki, Y. Harada, H. Hirohashi, Y. Watanabe, Y. Sakisaka, and H. Kato, *Phys. Rev. Lett.* **71,** 4214 (1993).
18. T. Arunarkavalli, G. U. Kulkarni, and C. N. R. Rao, *J. Solid State Chem.* **107,** 299 (1993).
19. M. Abbate, J. C. Fuggle, A. Fujimori, L. H. Tjeng, C. T. Chen, R. Potze, G. A. Sawatzky, H. Eisaki, and S. Uchida, *Phys. Rev. B* **47,** 16124 (1993).
20. S. R. Barman and D. D. Sarma, *Phys. Rev. B* **49,** 13979 (1994).
21. J. B. Goodenough, J-S. Zhou, and J. Chan, *Phys. Rev. B* **47,** 5275 (1993).
22. R. J. H. Voorhoeve, D. W. Johnson, Jr., J. P. Remeika, and P. K. Gallagher, *Science* **195,** 827 (1977).
23. G. Demazeau, M. Pouchard, and P. Hagenmüller, *J. Solid State Chem.* **9,** 202 (1974).